

ITEP-TH-36/98
KANAZAWA-98-08
UL-NTZ 18/98

September 10, 1998

Z -Vortex Percolation in the Electroweak Crossover Region

M. N. Chernodub^{1,a}, F. V. Gubarev^{2,a}, E.-M. Ilgenfritz^{3,b}
and A. Schiller^{4,c}

^a *ITEP, B. Cheremushkinskaya 25, Moscow, 117259, Russia*

^b *Institute for Theoretical Physics, Kanazawa University,
Kanazawa 920-1192, Japan*

^c *Institut für Theoretische Physik and NTZ, Universität Leipzig,
D-04109 Leipzig, Germany*

Abstract

We study the statistical properties of Z -vortices and Nambu monopoles in the 3D $SU(2)$ Higgs model for a Higgs mass $M_H \approx 100$ GeV where they are thermally created near to the crossover temperature and above. Although there is no phase transition at that strong selfcoupling, we observe that the Z -vortices exhibit the *percolation* transition that has been found recently to accompany the first order thermal transition that exists at smaller Higgs mass. At higher temperature percolating networks of Z -vortex lines are ubiquitous, whereas vortices are forming a dilute gas of closed vortex loops and of (Nambu) monopolium states on the low-temperature side of the crossover. The percolation temperature turns out to be approximately independent of the lattice spacing. We find the Higgs field modulus smaller (the gauge field action larger) inside the vortices, compared to the bulk average. This correlation becomes very strong on the low-temperature side. A percolation transition like this would be a prerequisite of string mediated baryon number generation scenarios in more realistic Higgs models.

¹chernodub@vxitep.itep.ru

²Fedor.Gubarev@itep.ru

³ilgenfri@hep.s.kanazawa-u.ac.jp

⁴schiller@tph204.physik.uni-leipzig.de

1 Introduction

According to recent lattice studies [1, 2, 3, 4] it is very likely that the standard electroweak theory does not pass a true phase transition at finite temperature. The 3D $SU(2)$ Higgs model as the effective, dimensionally reduced version of electroweak theory with a t -quark of appropriate mass, ceases to possess a first order transition for a Higgs mass $M_H > 72$ GeV. At larger values of Higgs mass the model investigated merely experiences a smooth crossover [5]. Due to the quantitative similarity of the phase transitions in the $SU(2)$ Higgs model and in the $SU(2) \times U(1)$ electroweak theory [6], respectively, and taking the current experimental lower bound [7] of the Higgs boson mass, $M_H \geq 89.3$ GeV, into account, the statement above is highly justified.

Within the most popular baryon number generation (BG) scenarios [8] even a *sufficiently strong* first order transition is required. Therefore the search for viable extensions of the standard model and the study of their phase structure has become an important direction of research. Nevertheless, last but not least in view of possible alternative BG mechanisms, it is still of some phenomenological interest to study features of the *standard model* which change qualitatively at some characteristic temperature (at the W mass scale). For instance, a changing spectrum of screening states could be the analogue of the phase transition that exists at lower Higgs mass. Very recently, we have shown [9] that the first order phase transition at $M_H \leq 70$ GeV is accompanied by a percolation transition^a experienced by some kind of topological defects. This issue is a very new one in the field of lattice studies of the electroweak transition, and various aspects have still to be clarified. In this paper we shall describe what remains from this percolation transition when the thermal phase transition changes into a rapid crossover.

This paper is the second of a series of studies we want to devote to the *statistical properties* of so-called *embedded* topological defects [11, 12] within the $SU(2)$ Higgs model. The embedded defects of interest are Nambu monopoles [13] and Z -vortices [13, 14]. Although not stable topologically, these defects are seen occurring as the result of thermal fluctuations. Here we are able to show that the percolation transition mentioned above persists at higher Higgs mass. For the first time we also provide evidence in this paper that Z -vortices are indeed characterized by inhomogeneities of gauge invariant quantities (gauge field action and Higgs field modulus) that have to be expected because of their appearance in the continuum.

Embedded topological defects might be important agents in some electroweak baryogenesis mechanisms. One of such scenarios is based on the decay of an electroweak string network as the Universe cools down. According to this mechanism, long electroweak strings should decay into smaller, twisted and linked string loops which carry non-zero baryon number. This could then explain the emergence of non-zero baryon number in the Universe [15]. We have nothing to contribute to this mechanism as such nor to the kinetics of such decaying network. In our paper we merely study the properties of the embedded strings as they pop up in thermal

^aThis is in an agreement with an observation of Ref. [10], made in a different context, that a percolation of strings is a good disorder parameter for a phase transition in field theory.

equilibrium of the $SU(2)$ Higgs model. Similarly to what we have found earlier in the symmetric phase (when it can be clearly separated by a first order transition at lower Higgs mass) our results show the existence of a percolating network on the high temperature side of the crossover with finite probability (at $T > T_{\text{perc}}$) while only smaller clusters occur below T_{perc} , however much more frequently than at lower Higgs mass. Some of these clusters have open ends occupied by Nambu monopoles. This suggests a BG scenario without a first order phase transition according to which a large vortex cluster might decay into small vortex pieces at some temperature.

On the lattice, a vortex cluster is a collection of dual links which are occupied by vortex trajectories (carry non-zero vorticity) and have common sites. A (connected) cluster cannot be decomposed into subclusters without cutting a dual link with non-zero vorticity. Mutually disconnected clusters are counted as several different clusters. The cluster length is the number of dual links forming a (connected) cluster.

Our investigation is performed in the framework of dimensional reduction which is expected to lend a reliable effective description of the $4D$ $SU(2)$ Higgs theory for Higgs masses between 30 and 240 GeV at temperatures of $O(100)$ GeV. Due to their relatively rich abundance on the low temperature side in the crossover region, the physics of distinct vortex loops and monopolium states (thought to be the remnants of the percolation cluster(s)) is sufficiently interesting to be studied more in detail and within the $4D$ Euclidean approach. Equally interesting would be the space-time structure of the vortex networks in the percolating phase. In our present $3D$ approach, we can get only some rough anticipation of what is going on in $4D$: the average $3D$ densities might be *time-projected* densities (describing the vortex network above or the small vortex clusters below the percolation temperature). In the $4D$ Euclidean version of the model the vortex lines we are studying would sweep out 2-dimensional world surfaces. The clusters of filamentary embedded vortex defects that we observe in the dimensionally reduced variant could be compactifications of or cuts through these world surfaces. Whatever the relation is, in the present paper, referring to the crossover region, we have for the first time studied the $3D$ cluster statistics (the number and length distributions) of the configurations.

The structure of the paper is as follows. We recall the effective, dimensionally reduced formulation of the electroweak theory as a $3D$ $SU(2)$ lattice Higgs model in Section 2. In this section, for the convenience of the reader, we also formulate the lattice definitions of the (elementary and extended) embedded topological defects proposed in Refs. [16, 9]. In Section 3 we present the numerical results on the density of Nambu monopoles and vortices and on the percolation probability of the corresponding Z -vortex lines in the crossover region. We show how the average number of lattice clusters (formed by vortex lines) and the average length (*i.e.* the number of dual links with non-zero vorticity) of vortex clusters changes at the transition. We also give some first results on gauge invariant signatures showing that the vortices provide a filamentary inhomogeneous structure of the system. Section 4 contains a short discussion of our results and conclusions.

2 Nambu Monopoles and Z-Vortices in the Lattice $SU(2)$ Higgs Model

For the investigation of the thermal equilibrium properties of the defects to be defined below we used the lattice 3D $SU(2)$ Higgs model with the following action:

$$S = \beta_G \sum_p \left(1 - \frac{1}{2} \text{Tr} U_p\right) - \beta_H \sum_{x,\mu} \frac{1}{2} \text{Tr} (\Phi_x^\dagger U_{x,\mu} \Phi_{x+\hat{\mu}}) + \sum_x \left(\rho_x^2 + \beta_R (\rho_x^2 - 1)^2 \right)$$

(the summation is taken over plaquettes p , sites x and links $l = \{x, \mu\}$). The action contains three parameters: the gauge coupling β_G , the lattice Higgs self-coupling β_R and the hopping parameter β_H . The gauge fields are represented by unitary 2×2 link matrices $U_{x,\mu}$ and U_p denotes the $SU(2)$ plaquette matrix. In this action, the Higgs field is parameterized as follows: $\Phi_x = \rho_x V_x$, where $\rho_x^2 = \frac{1}{2} \text{Tr} (\Phi_x^\dagger \Phi_x)$ is the Higgs modulus squared, and V_x an element of the group $SU(2)$. Later on, the 2×2 matrix-valued Higgs field Φ_x is replaced by the more standard isospinor notation $\phi_x = (\Phi_x^{11}, \Phi_x^{21})^T$.

The lattice parameters are related to the couplings of the 3D superrenormalizable $SU(2)$ Higgs model in the continuum, g_3 , λ_3 and m_3 ($\mu_3 = g_3^2$) as given *e.g.* in [1]. As in [1] a parameter M_H^* is used (approximately equal to the zero temperature physical Higgs mass) to parameterize the Higgs self-coupling as follows:

$$\beta_R = \frac{\lambda_3}{g_3^2} \frac{\beta_H^2}{\beta_G} = \frac{1}{8} \left(\frac{M_H^*}{80 \text{ GeV}} \right)^2 \frac{\beta_H^2}{\beta_G}. \quad (1)$$

Lattice coupling β_G and continuum coupling g_3^2 are related by

$$\beta_G = \frac{4}{ag_3^2}, \quad (2)$$

with a being the lattice spacing. We have studied the model at different gauge couplings β_G in order to qualitatively understand the appearance on the lattice of embedded defects of some characteristic physical size using lattices with different lattice spacing such that, eventually, the continuum limit can be accessed. This requires to define operators which count extended defects of arbitrary size in lattice units.

Let us first recall the definition of the elementary topological defects. The gauge invariant and quantized lattice definition [16] of the Nambu monopole is closely related to the definition in the continuum theory [13]. First we define a composite adjoint unit vector field $n_x = n_x^a \sigma^a$, $n_x^a = -(\phi_x^\dagger \sigma^a \phi_x) / (\phi_x^\dagger \phi_x)$ with σ^a being the Pauli matrices. In the following construction, the field n_x plays a role similar to the direction of the adjoint Higgs field in the definition of the 't Hooft–Polyakov monopole [17] in the Georgi–Glashow model. Here it is used to define the gauge invariant flux $\bar{\theta}_p$ carried by the plaquette p ,

$$\bar{\theta}_p(U, n) = \arg \left(\text{Tr} \left[(\mathbb{1} + n_x) V_{x,\mu} V_{x+\hat{\mu},\nu} V_{x+\hat{\nu},\mu}^\dagger V_{x,\nu}^\dagger \right] \right), \quad (3)$$

in terms of projected links

$$V_{x,\mu}(U, n) = U_{x,\mu} + n_x U_{x,\mu} n_{x+\hat{\mu}}.$$

In the unitary gauge, with $\phi_x = (0, \varphi)^T$ and $n_x^a \equiv \delta^{a3}$, the phases $\theta_l^u = \arg U_l^{11}$ behave as a compact Abelian field with respect to the residual Abelian gauge transformations $\Omega_x^{abel} = e^{i\sigma_3 \alpha_x}$, $\alpha_x \in [0, 2\pi)$ which leave the unitary gauge condition intact. Instead of in terms of the plaquettes θ_p of this Abelian field, the magnetic charge of Nambu monopoles - the topological defects of this Abelian field - can alternatively be defined using a gauge invariant construction [16]. The monopole charge j_c carried by the cube c can be expressed in terms of the gauge invariant fluxes (3) passing through the surface ∂c :

$$j_c = -\frac{1}{2\pi} \sum_{p \in \partial c} \bar{\theta}_p, \quad \bar{\theta}_p = (\theta_p - 2\pi m_p) \in [-\pi, \pi). \quad (4)$$

The Z -string [14, 13] corresponds to the Abrikosov–Nielsen–Olesen vortex solution [18] embedded [11, 12] into the electroweak theory^b. The Z -vorticity number corresponding to the plaquette $p = \{x, \mu\nu\}$ is defined [16] as follows:

$$\sigma_p = \frac{1}{2\pi} (\chi_p - \bar{\theta}_p), \quad (5)$$

where $\bar{\theta}_p$ has been given in (3), and $\chi_p = \chi_{x,\mu\nu} = \chi_{x,\mu} + \chi_{x+\hat{\mu},\nu} - \chi_{x+\hat{\nu},\mu} - \chi_{x,\nu}$ is the plaquette variable formed in terms of the Abelian links

$$\chi_{x,\mu} = \arg(\phi_x^\dagger V_{x,\mu} \phi_{x+\hat{\mu}}).$$

The Z -vortex is formed by links $l = \{x, \rho\}$ of the dual lattice which are dual to those plaquettes $p = \{x, \mu\nu\}$ which carry a non-zero vortex number (5): $^*\sigma_{x,\rho} = \varepsilon_{\rho\mu\nu} \sigma_{x,\mu\nu} / 2$. One can show that Z -vortices begin and end on the Nambu (anti-) monopoles: $\sum_{\mu=1}^3 (^*\sigma_{x-\hat{\mu},\mu} - ^*\sigma_{x,\mu}) = ^*j_x$.

In order to understand the behavior of the embedded defects towards the continuum limit we studied also numerically so-called *extended* topological objects on the lattice according to Ref. [19]. A similar approach has been pursued in Ref. [20], in which lattice vortices of extended size have been studied in the non-compact version of the 3D Abelian Higgs model. An extended monopole (vortex) of physical size $k a$ is defined on k^3 cubes (k^2 plaquettes, respectively). The charge of monopoles $j_{c(k)}$ on bigger k^3 cubes $c(k)$ is constructed analogously to that of the elementary monopole, eq. (4), with the elementary 1×1 plaquettes in terms of $V_{x,\mu}$ replaced by $n \times n$ Wilson loops (extended plaquettes). In the context of pure gauge theory, in the maximally Abelian gauge, this construction is known under the name of type-I extended objects. For the present model an alternative construction (type-II),

^bNote that there are two independent vortex solutions in the electroweak theory: Z -vortex and W -vortex, see Ref. [12]. In the limit of zero Weinberg angle θ_W (which is considered in the present paper) both solutions coincide up to a global gauge transformation. If $\theta_W \neq 0$ our construction (5) of the Z -vortex should be properly modified and complemented by one of the W -vortex. In fact, (5) would then correspond to what is called there a W -vortex solution.

obtained by blocking elementary topological objects, fails to lead to a good continuum description [9]. A more detailed definition of extended Nambu monopoles and Z -vortices can be found in Ref. [9].

3 Defect Dynamics at the Crossover

3.1 Density and Percolation

First, we study the behavior of *elementary* Nambu monopoles and Z -vortices along a line in parameter space passing through the continuous crossover region. Monte Carlo simulations have been performed on cubic lattices of size $L^3 = 16^3$ at $\beta_G = 12$ for self-couplings λ_3 corresponding to a Higgs mass $M_H^* = 100$ GeV, see eq. (1). In our simulations we used the algorithms described in Ref. [1] which combine Gaussian heat bath updates for the gauge and Higgs fields with several reflections for the fields to reduce the autocorrelations. We varied the parameter β_H in order to traverse the region of the crossover at given M_H^* and β_G .

At this stage we were interested in the behavior of the lattice Nambu monopole (ρ_m) and Z -vortex (ρ_v) densities and of the percolation probability C for the Z -vortex as functions of β_H . For each lattice configuration, the densities ρ_m and ρ_v are given by

$$\rho_m = \frac{1}{L^3} \sum_c |j_c|, \quad \rho_v = \frac{1}{3L^3} \sum_p |\sigma_p|,$$

where c and p refer to elementary cubes and plaquettes; the monopole charge j_c and the Z -vorticity σ_p are defined in (4) and (5), respectively.

The percolation probability of the system of vortex lines $^*\sigma$ (which typically can be decomposed into several mutually disconnected lattice clusters) is defined as a limit of the following two-point function [21]:

$$C = \lim_{r \rightarrow \infty} C(r), \tag{6}$$

$$C(r) = \left(\sum_{x,y,i} \delta_{x \in ^*\sigma^{(i)}} \delta_{y \in ^*\sigma^{(i)}} \cdot \delta(|x - y| - r) \right) \cdot \left(\sum_{x,y} \delta(|x - y| - r) \right)^{-1},$$

where the summation is taken over all points x, y of the dual lattice with fixed distance and over all connected clusters $^*\sigma^{(i)}$ of links carrying vorticity (i labels distinct vortex clusters). The Euclidean distance between two points x and y is denoted as $|x - y|$. The notation $x \in ^*\sigma^{(i)}$ means that the vortex world line cluster $^*\sigma^{(i)}$ passes through the point x . Connected clusters $^*\sigma^{(i)}$ are called percolating clusters if they contribute to the limit C .

Formula (6) corresponds to the thermodynamical limit. In our finite volume we find numerically that the function $C(r)$ can be fitted as $C(r) = C + C_0 r^{-\alpha} e^{-mr}$, with C, C_0, α and m being fitting parameters. As we observed, $m \sim a^{-1}$ in the explored region of the phase diagram, therefore we can be sure that finite size corrections to C are exponentially suppressed. If C does not vanish on an infinite lattice then

the vacuum is populated by one or more percolating clusters, each consisting of *infinitely many* dual links with non-vanishing vorticity. This implies the existence of a non-vanishing vortex condensate. If C turns to zero the vortex condensate vanishes according to this definition.

In Figure 1(a) we show the ensemble averages of densities, $\langle \rho_m \rangle$ of Nambu monopoles and $\langle \rho_v \rangle$ of Z -vortices as a function of the hopping parameter β_H for Higgs mass $M_H^* = 100$ GeV at gauge coupling $\beta_G = 12$. Both densities vanish very smoothly with increasing hopping parameter β_H , (which corresponds to a decreasing physical temperature). The percolation probability shown in Figure 1(b) vanishes at some value of the coupling constant β_H corresponding to a percolation temperature well above the temperature where the densities turn to zero. In fact, the percolation ends while the density of monopoles and vortices still amounts to some fraction of the densities of these objects deep in the symmetric phase.

We interpret this by an analogy according to which the would-be Higgs phase in the crossover region (at temperatures below some crossover temperature) resembles a type II superconductor in so far as it can support thick vortices which cannot form infinite clusters. In Nature, in a real cooling process passing the crossover, the percolating cluster(s) that has (have) existed above the crossover temperature would have been broken into vortex rings or vortex strings connecting Nambu monopole pairs.

It would be tempting to identify the crossover temperature with the percolation temperature if the latter has a well-defined meaning in the continuum limit. In order to explore whether the percolation effect persists approaching the continuum limit we have studied also extended topological objects (using the so-called type-I construction mentioned in Section 2). According to (2) the physical size of the k^3 monopoles (or the k^2 vortices) in simulations done at $\beta_G = k \beta_G^{(0)}$ should be roughly the same for all k . Since we expect finite volume effects to be potentially more severe at $M_H^* = 100$ GeV than at a strongly first order phase transition we were careful to keep also the physical size of the lattice fixed: at $\beta_G = k \beta_G^{(0)}$ we have performed simulations on lattices with a volume $(k L_0)^3$, respectively.

For the coarsest lattice we have chosen $\beta_G = \beta_G^{(0)} = 8$ and $L = L_0 = 16$. We show the behavior of the percolation probability near the crossover point on Figures 2(a,b,c) for $k = 1, 2, 3$, respectively. One can clearly see the existence of a percolation transition for each vortex size k . The actual value of the coupling β_H^{perc} corresponding to the percolation transition varies with k , similar to how β_H^{trans} was observed to change with β_G and L^3 at smaller Higgs mass (when there is a true first order phase transition). Also here, one can analogously define a physical percolation temperature T^{perc} corresponding to β_H^{perc} . This temperature is found to become roughly independent of β_G (or the lattice spacing) with decreasing lattice spacing. That means that the defects popping up dynamically (as well as the corresponding percolation temperature) become increasingly well-defined when the lattice becomes fine-grained enough to resolve the embedded vortices as extended objects. This indicates that the percolation temperature has a good chance to possess a well-defined continuum limit. Taking into account the perturbative relations between

3D and 4D quantities [22], T^{perc} can be roughly estimated as 170 GeV or 130 GeV, dependent on which version of the 4D continuum $SU(2)$ -Higgs theory is represented by the effective model, without fermions or with fermions including the top quark. The corresponding zero temperature Higgs mass M_H would be 94 and 103 GeV in the respective theories.

Notice however that for the finer lattices (bigger vortex size in lattice units) there appears a tail of small percolation probability before C finally turns to zero. This means that, still above the percolation temperature, the percolating clusters become more dilute, only a part of the lattice configurations actually contains a percolating cluster ("intermittent" percolation), and more and more smaller clusters appear.

3.2 Cluster Statistics

In order to look closer for the properties of the small vortex loops that populate the low temperature side of the crossover at not too low temperature, we have also measured the Monte Carlo ensemble average of the number of mutually disconnected clusters per configuration and the average length per (connected) cluster. The behavior of these quantities for different $k = 1, 2, 3$ are qualitatively the same, therefore we present these quantities for the case of extension parameter $k = 2$. We show in Figure 3 results obtained for the corresponding lattice size 32^3 and gauge coupling $\beta_G = 16$: (a) the density of the Nambu monopoles and Z -vortices, (b) the average length \mathcal{L} per Z -vortex cluster and (c) the average number \mathcal{N} of mutually disconnected Z -vortex clusters per lattice configuration.

It is clearly seen from Figure 3(a) that at the percolation transition (compare Figure 2(b) for $k = 2$ at $\beta_H^{\text{perc}} \approx 0.3432$) the density of monopoles and vortices decreases smoothly with increasing β_H . From Figure 3(b) one can conclude that the average length of the vortex clusters \mathcal{L} decreases drastically while the number of vortex clusters \mathcal{N} increases sharply (Figure 3(c)) already at somewhat smaller β_H . The latter reaches its maximum at β_H^{perc} . With the help of equation (2) and $g_3^2 \approx g_4^2 T \approx 0.43T$ we get, choosing $k = 2$ and $\beta_G = 16$ as an example, a lattice spacing $a = 1/(300 \text{ GeV})$. We can estimate the densities of $k = 2$ Nambu monopoles and Z -vortices in physical units. At the percolation temperature 170 GeV we get, for lattice densities $\rho_v = 0.14$ and $\rho_m = 0.26$, in the continuum a vortex density of $(55 \text{ GeV})^2$ and a monopole density of $(93 \text{ GeV})^3$. Taking into account that, classically, the core widths of embedded defects are of the order of M_W^{-1} we conclude that vortices and monopoles are densely packed at the percolation transition and, as a result, their cores are strongly overlapping. After the percolation transition is completed, the open or closed vortex strings are very short: their mean length is roughly three times the classical vortex width. The average cluster length amounts to $5ka = 1/(30 \text{ GeV})$.

Although these results characterize structures formed by thermal fluctuations within equilibrium thermodynamics, all facts suggest strongly that in a non-equilibrium cooling process the percolating cluster(s) and other bigger clusters decay near to the percolation temperature T^{perc} , primarily into small closed vortex loops which later gradually shrink and disappear with further decreasing of temperature

(increasing of β_H). The detailed dynamics of this process requires thorough investigations using non-equilibrium techniques.

Note that even at β_H values far above the percolation point there is a long plateau in the average length per vortex clusters at a level of $\mathcal{L} \approx 2$. A more detailed analysis of the field configurations shows in fact that here, below the percolation temperature, each configuration contains a large number (a few dozen, according to Figure 3(c)) of monopole–anti-monopole pairs connected by vortex trajectories of length 1 – 2 and only few additional closed vortex loops. As it was shown in Ref. [16] the sphaleron configuration (an unstable solution to classical equations of motion) contains in its center a monopole–anti-monopole pair connected by a short vortex string. It is suggestive to interpret the open Z –vortex strings (which exist within some temperature interval below the percolation temperature with a small density) as sphalerons.

3.3 Z –Vortices as Physical Objects

In this Subsection we show that our construction of the Z –vortices on the lattice (5) defines objects resembling some characteristic features of the classical Z –vortex solutions in continuum. Our construction detects a line-like object with non-zero vorticity and there is no guarantee that this configuration has a particular vortex profile. However, as we show below, the lattice Z –vortices have some common features with the classical solutions.

At the center of a classical continuum Z –vortex the Higgs field modulus is zero and the energy density reaches its maximum [13, 12]. If the vacuum is populated by vortex-like configurations then it would be natural to expect that along the axis of these configurations there will be a line of zeroes of the Higgs field and of points with maximal energy density. The simplest way to test how good this expectation is fulfilled is to measure the (squared) modulus of the Higgs field and the energy density near the dual vortex-carrying links defined by (5) and compare these quantities with the corresponding bulk average values far from the vortex core^c.

Here we restrict ourselves to the case of elementary defects. This is the worst case in the sense that it obviously does not allow to define a profile of a defect resembling the continuum case. We will come back to the profile of an extended defect in a forthcoming publication. For the present purposes the non-vanishing of (5) is simply used as a trigger to measure the above mentioned observables. We define the mean value of the modulus squared of the Higgs field inside the (elementary) vortex, $\langle \rho^2 \rangle_{\text{in}}$, as the average of $(\phi_x^+ \phi_x)$ over the corners of *all* plaquettes with $\sigma_P \neq 0$ (dual to the vortex-carrying links). For simplicity, the analogous quantity outside the (elementary) vortex, $\langle \rho^2 \rangle_{\text{out}}$, is obtained as the corresponding average over the corners of *all* plaquettes with $\sigma_P = 0$. Even more straightforward is the definition of the corresponding averages of the gauge field energy as volume averages of $1 - \frac{1}{2}\text{Tr}U_P$ depending on whether σ_P is equal to or different from zero.

^cA similar method has been used to study the physical features of the Abelian magnetic monopoles in non-Abelian gauge theories in Ref. [23].

The quantities $\langle \rho^2 \rangle_{\text{in,out}}$ are plotted *vs.* β_H for $\beta_G = 8$ in Fig. 4(a). One can clearly see that the modulus of the Higgs field is smaller near to the vortex trajectory than outside the vortex for all values of the coupling β_H . In order to make clearer the different behavior of the quantities $\langle \rho^2 \rangle_{\text{in,out}}$ on both sides of the crossover we show in Fig. 4(b) the histograms of these quantities on the symmetric side ($\beta_H = 0.348$) and the Higgs side ($\beta_H = 0.356$).

On the symmetric side of the crossover (smaller β_H) the difference^d between quantities $\langle \rho^2 \rangle_{\text{in,out}}$ is much smaller than on the Higgs side (larger β_H). This fact is natural, since on the symmetric side the vortices densely populate the vacuum and vortex cores are overlapping while on the Higgs side of the transition the vortices are dilute. The value of the Higgs field modulus in the region between closely placed vortices is smaller than between far separated vortices. As to be expected for elementary lattice vortices, $\langle \rho^2 \rangle_{\text{in}}$ does not vanish. This is due to the relatively large lattice spacing which prevents that the Higgs field can be measured arbitrarily near to the vortex axis. A detailed study of the vortex profile (and a localization of the Higgs zeroes) requires the extended vortex construction and is under investigation [24].

The gauge field energies $\langle 1 - U_P \rangle_{\text{in,out}}$ are plotted *vs.* β_H in Fig. 4(c), the corresponding histograms are shown in Fig. 4(d) for the symmetric side ($\beta_H = 0.348$) and the Higgs side ($\beta_H = 0.356$) of the crossover. Both figures show that the value of the gauge field energy near to the vortex center is larger than in the bulk on both sides of the crossover.

The results of this Subsection clearly show that Z -vortices are physical objects and resemble the features of the classical continuum vortex solutions: vortices carry excess gauge field energy and the Higgs modulus decreases near to the vortex center.

4 Discussion and Conclusions

Recently we have started to investigate numerically the behavior of Nambu monopoles and Z -vortices in the $SU(2)$ Higgs model at high temperatures within the dimensional reduction approach. This model is used as representative for the standard model. Here we have extended our previous work to a region of Higgs mass where the model is known not to have a true thermal phase transition. We show that at large but not unrealistic Higgs mass $M_H \approx 100$ GeV the 3D percolation transition of the Z -vortex lines still exists that we have recently found to be a companion of the first order phase transition at lower mass. At temperatures below $T^{\text{perc}} \approx 170$ GeV (≈ 130 GeV for the more realistic case with the top quark included) space is densely populated by large vortex clusters with one or few infinitely extended ones among them. This state is not thermodynamically relevant at lower temperature. Instead of very large clusters, a gas containing of closed vortex loops and monopolium bound states (Nambu monopole–anti-monopole pairs bound by Z -strings) prevails.

^dNote, that only the difference between quantum averages of the squared modulus of the Higgs field (not the quantum average itself!) may be related to the continuum limit due to an additive renormalization, see Ref. [20] for a detailed discussion on this point.

Further below T^{perc} , with decreasing temperature small vortex loops shrink and disappear while monopole–anti-monopole pairs still survive. In the spirit of our recent investigation of classical sphaleron configurations we would associate these pairs with sphaleron-like configurations known to exist in the broken phase. Without going into details of specific mechanisms, we want to point out that the non-equilibrium break-up of infinitely extended electroweak vortex clusters into small closed loops with decreasing temperature is a prerequisite of string-mediated baryon number generation scenarios [15]. It is interesting to see that similar defect structures are realized within our effective Higgs model.

Acknowledgments

M. N. Ch. is grateful to L. McLerran, M. I. Polikarpov and K. Rummukainen for interesting discussions.

M. N. Ch. and F. V. G. were partially supported by the grants INTAS-96-370, INTAS-RFBR-95-0681, RFBR-96-02-17230a and RFBR-96-15-96740.

References

- [1] M. Gürtler *et al.*, *Nucl. Phys.* **B483** 383 (1997).
- [2] M. Gürtler, E.–M. Ilgenfritz and A. Schiller, *Phys. Rev.* **D56** (1997) 3888.
- [3] K. Rummukainen *et al.*, *preprint CERN-TH-98-08*, [hep-lat/9805013](#).
- [4] M. Laine and K. Rummukainen, talk given at the XVI International Symposium on Lattice Field Theory, Boulder, Colorado, 13-18 July, 1998; [hep-lat/9809045](#),
- [5] K. Kajantie *et al.*, *Phys. Rev. Lett.* **77** (1996) 2887.
- [6] K. Kajantie *et al.*, *Nucl. Phys.* **B493** (1997) 413.
- [7] S. de Jong, “*Higgs Searches at LEP*”, Review talk delivered at the XXXIIIrd Rencontres de Moriond, Les Arcs, France, March 14 – 21 (1998) .
- [8] A. D. Sakharov, *JETP Lett.* **6** (1967) 24; See also reviews: V. A. Rubakov and M. E. Shaposhnikov *Phys. Usp.* **39** (1996) 461; M. Trodden, *preprint CWRU-P6-98*, [hep-ph/9803479](#).
- [9] M. N. Chernodub, F. V. Gubarev, E.–M. Ilgenfritz and A. Schiller, *preprints ITEP-TH-12/98*, *KANAZAWA-98-03*, *ZIF-MS-30/98*, [hep-lat/9805016](#), *Phys. Lett.* **B** (in press).
- [10] N. D. Antunes, L. M. A. Bettencourt and M. Hindmarsh, *Phys. Rev. Lett.* **80** (1998) 908.
- [11] T. Vachaspati and M. Barriola, *Phys. Rev. Lett.* **69** (1992) 1867.
- [12] M. Barriola, T. Vachaspati and M. Bucher, *Phys. Rev.* **D50** (1994) 2819.
- [13] Y. Nambu, *Nucl. Phys.* **B130** (1977) 505.

- [14] N. S. Manton, *Phys. Rev.* **D28** (1983) 2019.
- [15] T. Vachaspati and G. B. Field, *Phys. Rev. Lett.* **73** (1994) 373; *ibid.* **74** (1995) *Errata*; “*Electroweak Strings, Sphalerons and Magnetic Fields*”, T. Vachaspati, in the Proceedings of the NATO Workshop on “*Electroweak Physics and the Early Universe*”, Sintra, Portugal (1994); Series B: Physics Vol. 338, Plenum Press, New York (1994); [hep-ph/9405286](#).
- [16] M. N. Chernodub, F. V. Gubarev and E.–M. Ilgenfritz, *Phys. Lett.* **B424** (1998) 106.
- [17] G. ‘t Hooft, *Nucl. Phys.* **B79** (1974) 276; A. M. Polyakov, *JETP Lett.* **20** (1974) 194.
- [18] A. A. Abrikosov, *Sov. Phys. JETP* **32** (1957) 1442; H. B. Nielsen and P. Olesen, *Nucl. Phys.* **B61** (1973) 45.
- [19] T. L. Ivanenko, A. V. Pochinskii and M. I. Polikarpov, *Phys. Lett.* **B252** (1990) 631.
- [20] K. Kajantie *et al.*, *Phys. Lett.* **B428** (1998) 334.
- [21] A. V. Pochinsky, M. I. Polikarpov and B. N. Yurchenko, *Phys. Lett.* **A154** (1991) 194; T.L. Ivanenko, A.V. Pochinskii and M.I. Polikarpov, *Phys. Lett.* **B302** (1993) 458; A. Hulsebos, [hep-lat/9406016](#); *Nucl. Phys. B (Proc. Suppl.)* **34** (1994) 695.
- [22] K. Kajantie *et al.*, *Nucl. Phys.* **B458** (1996) 90.
- [23] B.L.G. Bakker, M.N. Chernodub and M.I. Polikarpov, *Phys. Rev. Lett.* **80** (1998) 30.
- [24] M. N. Chernodub, F. V. Gubarev, E.–M. Ilgenfritz and A. Schiller, in preparation.

Figures

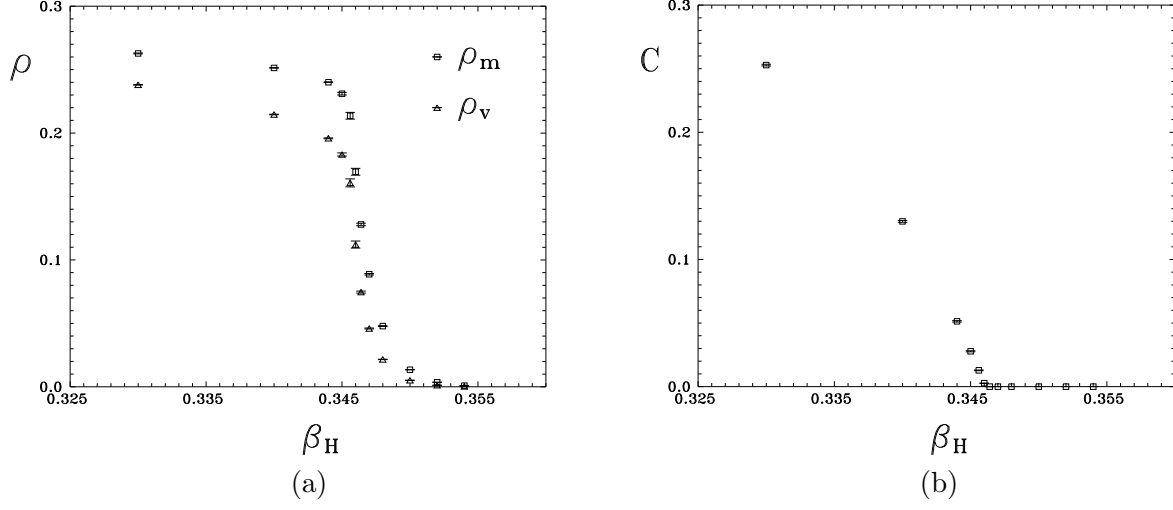


Figure 1: (a) Density ρ_m of Nambu monopoles and ρ_v of Z -vortices *vs.* hopping parameter β_H for Higgs mass $M_H^* = 100$ GeV at gauge coupling $\beta_G = 12$; (b) Percolation probability C of Z -vortex trajectories for the same parameters; the percolation transition happens at critical $\beta_H^{\text{perc}} \approx 0.3451$.

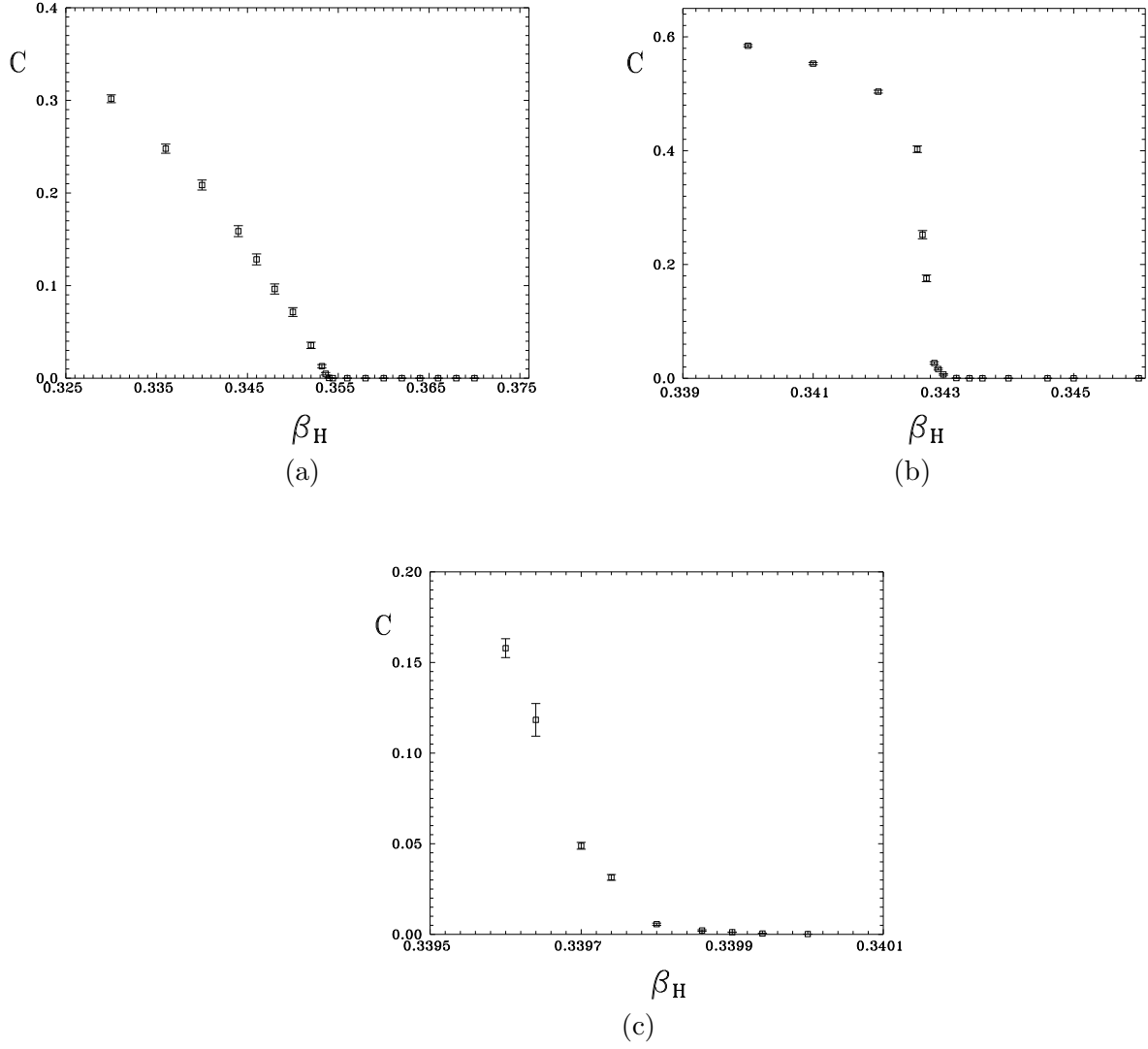


Figure 2: Percolation probability C *vs.* β_H for Z -vortices of size k^2 on lattices $(16k)^3$ at gauge couplings $\beta_G = 8k$, respectively, for (a) $k = 1$, (b) $k = 2$ and (c) $k = 3$.

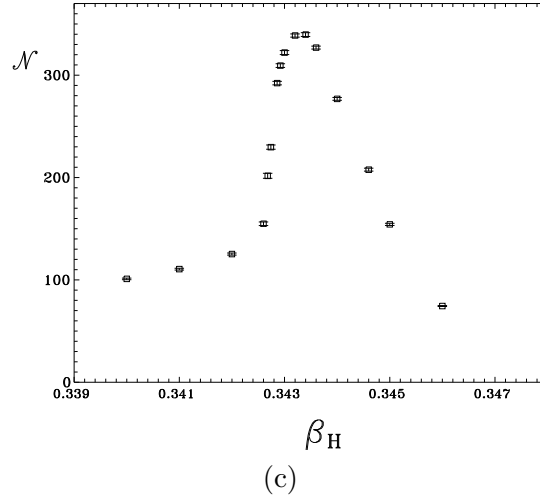
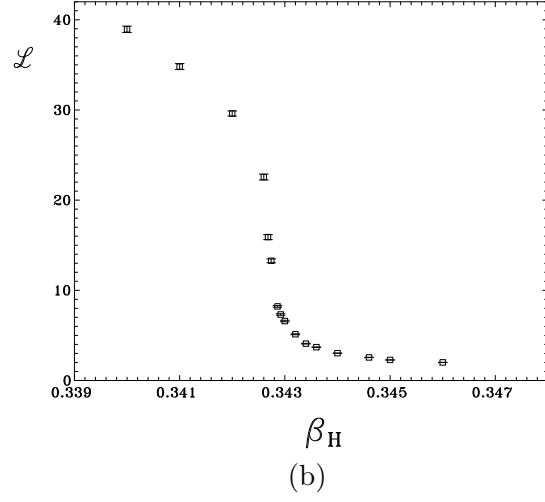
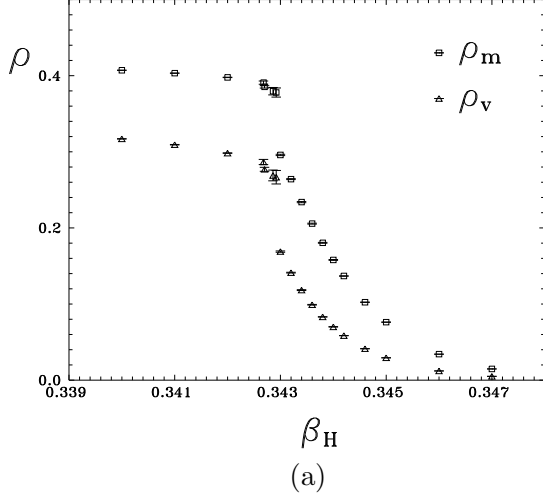


Figure 3: (a) Density ρ_m of Nambu monopoles and ρ_v of Z -vortices, (b) average length \mathcal{L} per Z -vortex cluster and (c) average number \mathcal{N} of mutually disconnected Z -vortex clusters per lattice configuration (all for size $k = 2$ objects with corresponding lattice size 32^3 and gauge coupling $\beta_G = 16$).

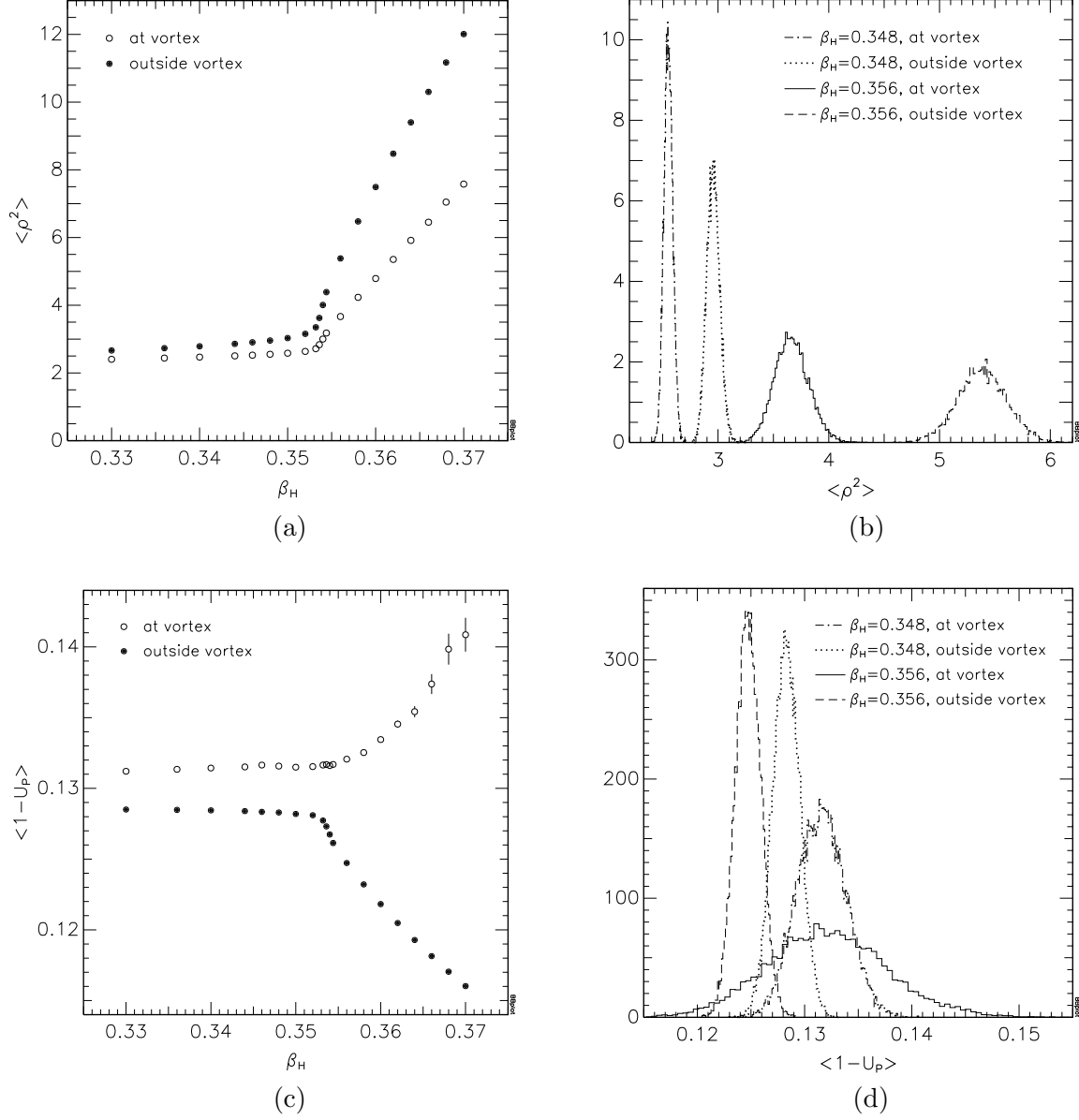


Figure 4: The squared Higgs modulus inside and outside of a Z -vortex: (a) *vs.* β_H ; (b) histograms on the symmetric ($\beta_H = 0.348$) and on the Higgs ($\beta_H = 0.356$) sides of the percolation transition. The same for gauge field energy: Figs. (c) and (d) respectively.